Journal of Solid Mechanics and Materials Engineering

Vol. 5, No. 1, 2011

Analysis of Separation Conditions for Shrink Fitting System Used for Ceramics Conveying Rollers*

Wenbin LI**, Nao-Aki NODA**, Hiromasa SAKAI** and Yasushi TAKASE**

** Department of Mechanical and Control Engineering, Kyushu Institute of Technology
Sensui-Cho 1-1 Tobata-Ku, Kitakyushu-Shi, Fukuoka, Japan
E-mail: noda@mech.kyutech.ac.jp

Abstract

Steel conveying rollers used in hot rolling mills must be exchanged frequently at great cost because hot conveyed strips induce wear and deterioration on the surface of roller in short periods. In this study, new roller structure is considered which has a ceramics sleeve connected with two steel shafts at both ends by shrink fitting. Here, although the ceramics sleeve can be used for many years, the steel shaft sometimes has to be exchanged for reconstruction under corrosive action induced by water cooling system. Since the thermal expansion coefficient of steel is about five times larger than that of ceramics, it is necessary to investigate how to separate the shrink fitting system by heating outside of sleeve and cooling inside of the shaft. In this study, the finite element method is applied to analyze the separation mechanism by varying the geometrical and thermal conditions for the structure. Finally the most appropriate dimension and thermal conditions have been found, which may be useful for designing of new rollers.

Key words: Thermal Deformation, Tool, Machine Element, Ceramics, Finite Element Method

1. Introduction

Conveying rollers in hot rolling mills as shown Fig.1 are usually made of cast iron alloy, carbon steel or alloy steel. Since they are used under high temperature and corrosive atmosphere, wear and deterioration are easily induced on the surface in a short period.

In this study, the new roller structure is considered which has a ceramics sleeve and two short steel shafts connected by shrink fitting at both ends, as shown in Fig.2 (b) [(1)]. Since the ceramics has high heat resistance and abrasion resistance [(2)], the exchanging cycle of roller can be extended in a large scale, and therefore, the reconstruction time and cost can be reduced. Moreover, the roller can be rotated easily and follow the speed of the transporting strips smoothly because of its light weight. In the previous study, the stress due to shrink fitting and stress due to load distribution were distinguished, and the effects of shrink fitting ratio, the fitted length, the material of sleeve and radius curvature upon those stresses were investigated.

Since the shafts are made of steel, it is necessary to exchange them frequently because hot conveyed strips induce wear and deterioration on the surface of roller in a short period. However, it should be noted that the linear expansion coefficient of steel is about five times as large as that of ceramics. In other words, since the steel expands more than ceramics, separation of the roller becomes difficult.

*Received 6 July, 2010 (No. 10-0281)
[DOI: 10.1299/jmmp.5.14]

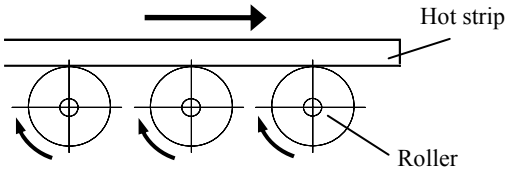

Fig.1 Layout of conveying rollers

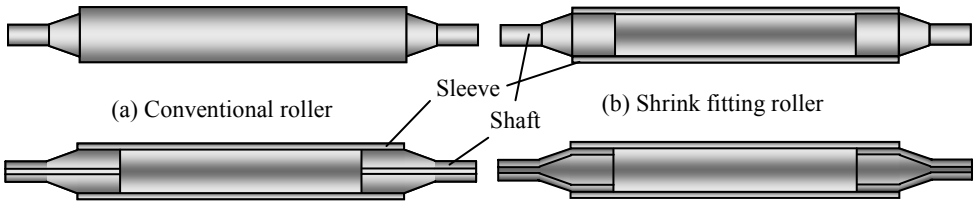

Fig.2 Roller structure

In this study, therefore, the structure shown in Fig.2 (c) and Fig.2 (d) will be considered, whose shafts has a hole for water cooling. In that case, the roller may be separated by heating outside surface of the ceramics sleeve and cooling inside surface of the steel shaft by water. Then, separation conditions will be investigated with varying dimensions by applying the finite element method. For reducing the cost, short separation time is desirable in industry.

2. Analytical Conditions

2.1 Boundary Conditions

Define the shrink fitting ratio as δ/d, where δ is the diameter difference with the diameter $d = 210mm$. Initially, the finite element method is applied to axisymmetric model A whose dimensions and boundary conditions are shown in Fig.3. The heating region is the outside surface of the contact part of sleeve as shown in Fig.3 (b). On the other hand, the water cooling region in Fig.3 (b) is the inside surface of the shaft, and the air cooling regions are the other regions including the left end surface of the shaft. In Fig.4, the assumed atmosphere temperature is shown according to the variation of a measured temperature in a furnace until the time 10000s. Then, forced convection as well as radiation is considered for heating. On the other hand, forced convection is assumed for water cooling, and natural convection for air cooling. Values of heat transfer coefficient α and emissivity ε for the present analysis are shown in Table 1 with Fig.5.

According to the symmetry of the problem, half model can be considered as shown in Fig.5. Therefore, along the surface $z = 0$ insulation is applied as the thermal boundary condition, and $u_z = 0$, $\tau_{rz} = 0$ are applied as mechanical boundary conditions. Similarly, at the right end of the shaft, insulation and $\sigma_z = 0$, $\tau_{rz} = 0$ are assumed. Along the contact surface between the sleeve and shaft, heat transmission is actually caused by solid thermal conduction through real contact area, and thermal conduction through fluid lying in the space between the nominal contact surfaces [3]. Since the contact stress due to shrink fitting is quite large, solid thermal conduction seems to be predominant. In this analysis, therefore, contact heat transfer coefficient is assumed as $1.0\times10^9\, W/m^2\cdot K$.

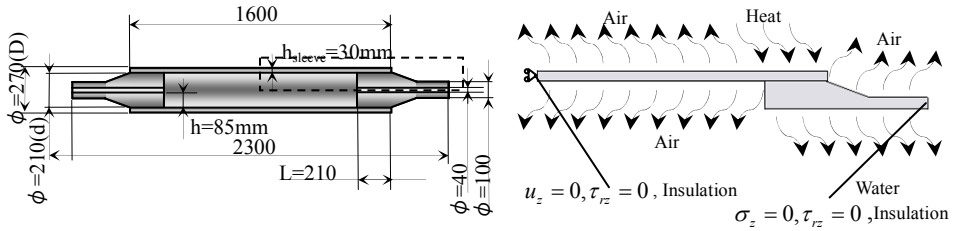

(a) Dimensions (mm) (b) Boundary condition

Fig.3 Model A initially considered

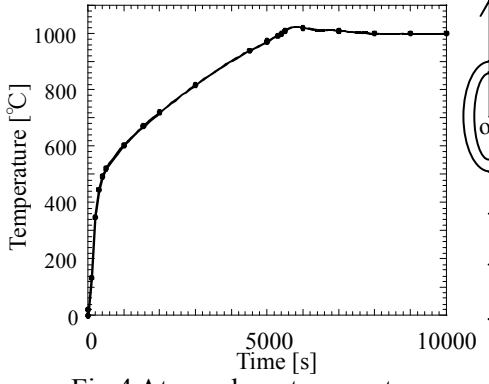

Fig.4 Atmosphere temperature

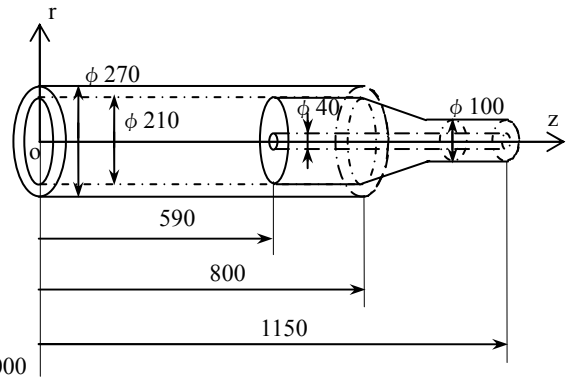

Fig.5 Model A with coordinate (mm)

Table1 Values of heat transfer coefficient α and emissivity ε along the r, z (mm) coordinate in Fig.5

Heat (Forced convection, Radiation)	r=135, z=±590~800 $\alpha = 50$ (W/m^2·K) $\varepsilon = 0.4$
Water cool (Forced convection)	r=20, z=±590~1150 $\alpha = 1.163\times10^4$ (W/m^2·K) $\varepsilon = 0$
Air cool (Natural convection)	r=105, z=0~±590 r=135, z=0~±590 r=20~105, z=±590 r=105~135, z=±800 r=50~105, z=±800~1150 (shaft surface) $\alpha = 50$ (W/m^2·K) $\varepsilon = 0$
Insulation	r=105~135, z=0 r=20~50, z=±1150

2.2 Material Properties

Table 2 shows the material properties of the roller. In this study, the steel shaft is considered with Vickers hardness $H_V = 200$. On the other hand, as the materials of the

Table2 Material properties

	Ceramics H	Ceramics I	Steel (H_V 200)
Young's modulus [GPa]	300	294	210
Poisson's ratio	0.28	0.27	0.3
Tensile strength [MPa]	500	500	600
Mass density [kg/m^3]	3200	3260	7800
Thermal conductivity [W/m·K]	62.5(393K) 12.5(1273K)	17(393K) 3.4(1273K)	25
Thermal expansion coefficient [1/K]	3.0×10^{-6}	3.0×10^{-6}	1.45×10^{-5}
Specific heat [J/kg·K]	680	650	477
Emissivity	0.4	0.4	0.4

sleeve, two kinds of Si_3N_4ceramics H and I are considered compared with a steel sleeve with $H_V = 200$. As shown in Table 2, it is assumed that the thermal conductivity of ceramics is linearly decreasing depending on the temperature. It should be noted that the thermal expansion coefficient of steel is about 5 times as large as that of ceramics. It is also noted that under most cases of temperature the heat conductivity of ceramics H is about four times as large as that of ceramics I.

2.3 Analytical Model

In this study, it is necessary to consider the thermal local deformations for sleeve and shaft in addition to heat transfer analysis for the whole structure. The thermal-mechanical coupled analysis is therefore performed for the models using quadrilateral axisymmetric element. As an example, the initial model A in Fig.2 (a) has 3894 elements and 4457 nodes. With the varying geometrical conditions, such as fitted length, and outside diameter of the sleeve, those effects on separation mechanism will be investigated with putting emphasis on the total heating and cooling time necessary for separation.

3. Results for Model A

3.1 Analysis of the Steel Sleeve Connected to Steel Shafts

First of all, a steel sleeve connected to steel shafts is analyzed to be compared with results of the ceramics sleeve. Figure 6 shows the relationship between separation time and shrink fitting ratio δ/d for steel sleeve. Here, the separation time is defined as the time when the displacement difference $\Delta u_r = u_r|_{r=(d/2)^+} - u_r|_{r=(d/2)^-}$ (d=210,365,480)in the radial direction becomes larger than the initial radial difference δ/d along the contact region. The separation starting time is the time when the first one point along the contact surface starts to be separated, while separation finishing time is the time when the whole contact part is separated completely. Naturally, when the shrink fitting ratio δ/d is small, both separation

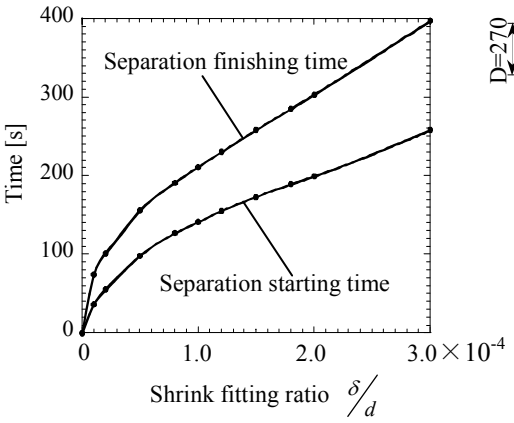

Fig.6 Time vs. δ/d for steel shaft and sleeve

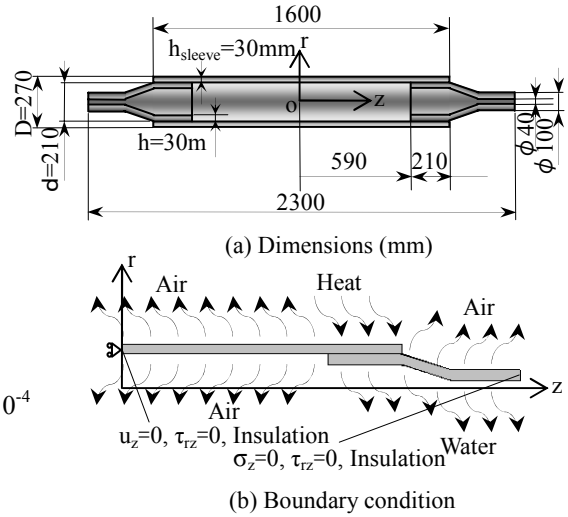

Fig.7 Roller model B

times are shorter. When $\delta/d < 1.0\times10^{-4}$, separation time rapidly increases with increasing δ/d, while the separation time almost increases linearly with increasing δ/d when $\delta/d \geq 1.0\times10^{-4}$.

3.2 Analysis of the Ceramics Sleeve Connected to Steel Shafts

Next, a ceramics sleeve connected to steel shafts is considered. However, in this case, we cannot see any separation point along the contact surface. In other words, because the expansion coefficient of the shaft is much larger than that of the sleeve, the shaft expands more than sleeve, and therefore no space can be generated along the contact surface. In order to make separation possible it is necessary to suppress the expansion of the shaft by reducing the temperature and cooling the shaft. As shown in Fig.3 (d), therefore, the new model B is considered. The thinner thickness of the shaft $h = 30mm$ has been applied to the fitted part of the shaft as shown in Fig.7. In addition, the signs and dimensions used are shown in Fig. 8.

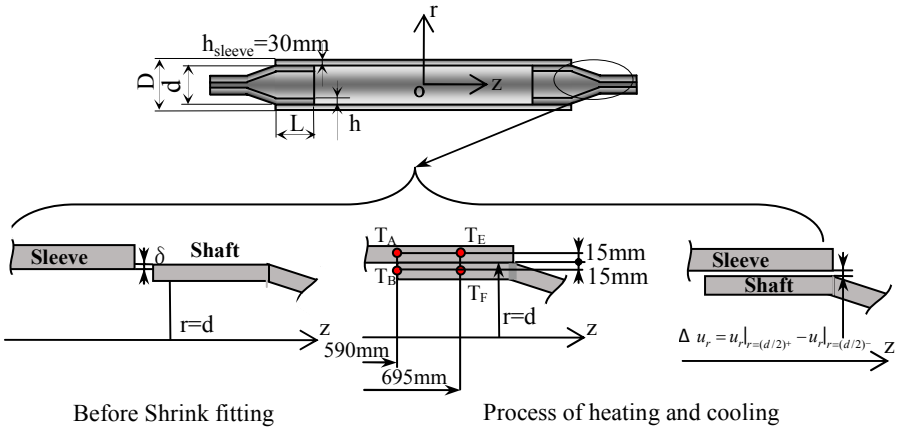

Fig.8 Relation of dimensions and signs

4. Results of Model B

4.1 The Effect of Shrink Fitting Ratio δ/d on Separation Time

By analyzing model B as shown in Fig.7, the separation can be realized successfully for ceramics sleeve and steel shaft. In the following study, therefore, a sleeve of ceramics H connected to steel shafts is mainly considered with focusing on the geometrical effects on the separation finishing time.

Initially, as shown in Fig. 9, three types of atmosphere temperatures are considered to confirm the heating effect on the final separation. Figure 10 shows the relationships between the separation time and shrink fitting ratio δ/d under the three types of atmosphere temperatures. The separation time is shorter for the temperature rising quickly, and longer for the temperature rising slowly. In the following discussion, the original atmosphere temperature in Fig. 9 is always used.

Figure 11 shows how the separation progresses along the contact area under different shrink fitting ratios. Separation starts from both ends of the shaft and extends to the inside. For small shrink fitting ratios, the last separation point is nearly in the middle of the contact region, while it moves to the right end of the sleeve when the shrink fitting becomes larger. Naturally, it is confirmed that separation time becomes longer as the shrink fitting ratio becomes larger. By the comparison between Fig.6 and Fig.10, it is seen that the separation time for ceramics H sleeve is about 10 times as long as that of steel sleeve when $\delta/d = 0.1\times10^{-3}$, while it is larger than 15 times when $\delta/d = 0.3\times10^{-3}$.

4.2 The Effect of Outside Diameter D on Separation Time

To investigate the effect of diameter, $D = 270mm$, $D = 405mm$, $D = 540mm$ are considered under a constant thicknesses of sleeve and shaft $h = 30mm$. Figure 12 shows separation time vs. shrink fitting ratio δ/d for different diameters. It is found that when the outside diameter becomes larger, separation time becomes shorter. In order to explain the results, the temperature difference between the sleeve and shaft at the end of the shaft $z = 590$ is investigated at the middle thickness of the sleeve and shaft. It should be noted that separation starts from the shaft end $z = 590mm$. Figure 13 shows the results for $D = 540mm$ and $D = 270mm$. Here, T_A, T_B represents the temperature of the middle in the thickness direction of the sleeve and shaft, T_A is $T_A(z,r) = T_A(590,120)$ when $D = 270mm$, and $T_A(z,r) = T_A(590,255)$ when $D = 540mm$; T_B is $T_B(z,r) = T_B(590,90)$ when $D = 270mm$, and $T_B(z,r) = T_B(590,225)$ when $D = 540mm$. The temperature difference $\Delta T = T_A - T_B$ is also shown in Fig. 13. Additionally, t_s represents separation starting time, while t_f represents for separation finishing time. According to Fig.13, the temperature of sleeve of $D = 540mm$ is much larger than that of $D = 270mm$, while the temperature of shaft of $D = 270mm$ is also larger than that of $D = 540mm$. Finally, the temperature difference of 540mm ΔT_{540} is larger that of 270mm ΔT_{270}. As shown in Fig. 13, the temperature difference at separation starting time for $D = 270mm$ and $D = 540mm$ is $9.5°C(318s)$

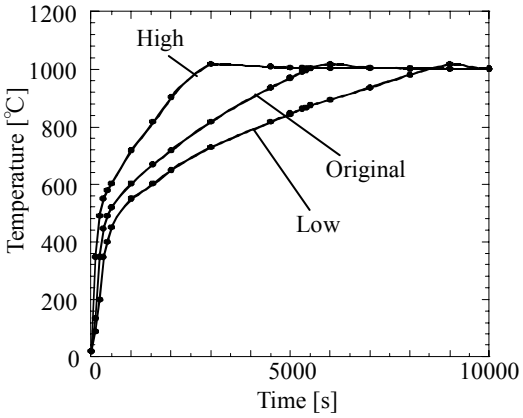

Fig.9 Each atmosphere temperature

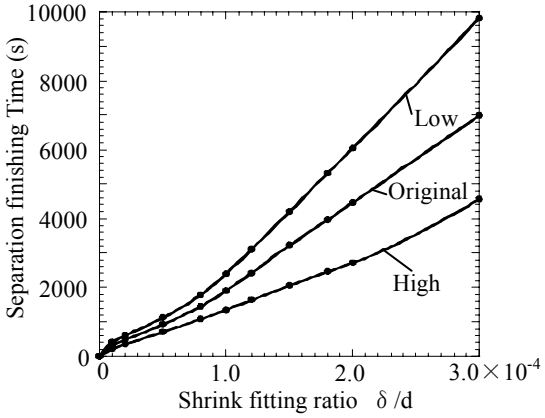

Fig.10 Time vs. δ/d for each atmosphere temperature

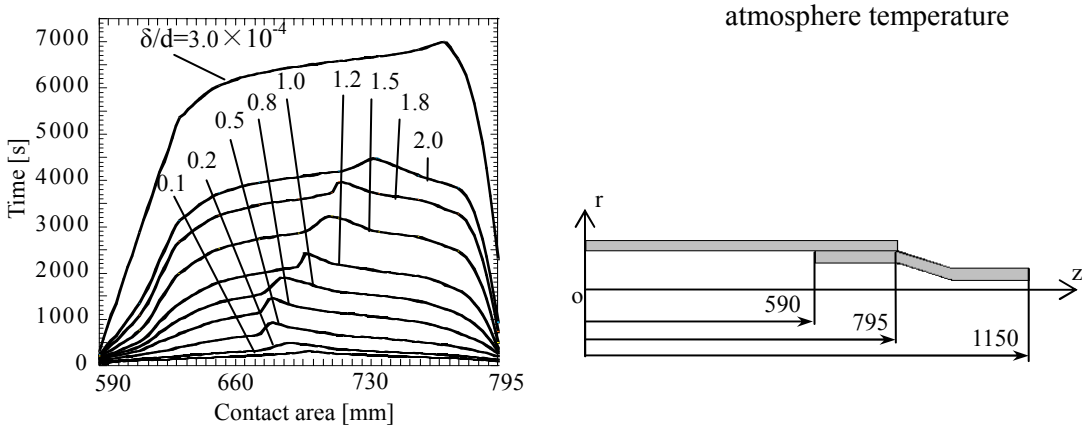

Fig.11 Separation history of Contact Area

and $5.3°C(215s)$ respectively, while at separation finishing time is $395°C(7009s)$ and $134°C(1621s)$ for $D = 270mm$ and $D = 540mm$ respectively.

Figure 14 shows the displacement difference $\Delta u_r = u_r\big|_{r=(d/2)^+} - u_r\big|_{r=(d/2)^-}$ in the r direction along the contact area for $D = 270mm$ and $D = 540mm$ at the same time 1000s after separation starting. In order to understand the separating condition easily, $\Delta u_r - \delta$ is also shown in Fig.14. It is seen that both separations start from both ends and the separation of $D = 540mm$ is earlier than that of $D = 270mm$. According to the discussions above, it is understood that separation time is shorter for a larger outside diameter of the sleeve.

4.3 The Effect of the Thickness of Shaft on Separation Time

By comparing the results of models A and B, it may be concluded that the separation is difficult for the large thickness h. Here, the effect of the shaft thickness is investigated more quantitatively. Here, the shaft thickness $h = 20mm, 30mm, 40mm$, are considered under the same sleeve thickness $h_{sleeve} = 30mm$. Figure 15 shows the relationship between the separation finishing time and shrink fitting ratio δ/d for different shaft thicknesses h.

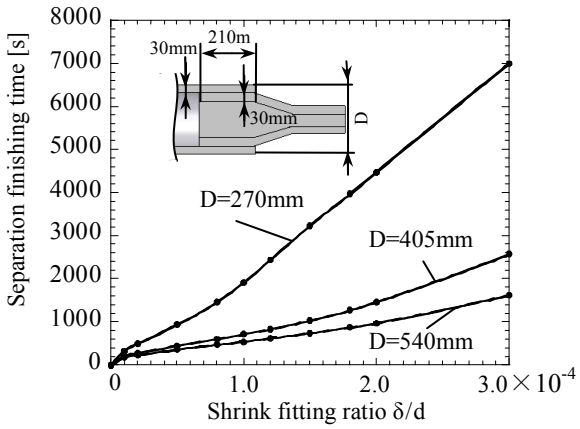

Fig.12 Time vs. δ/d for D=270mm, 405mm, 540mm

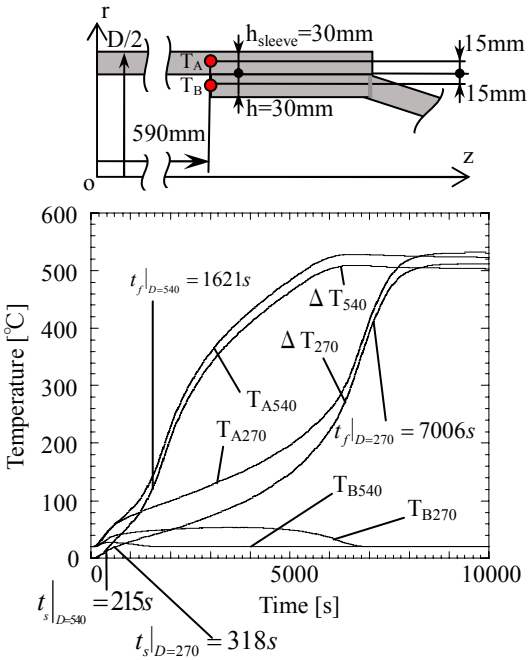

Fig.13 T_A, T_B and ΔT vs. Time for D=270mm, 540mm ($\delta/d = 3.0\times10^{-4}$)

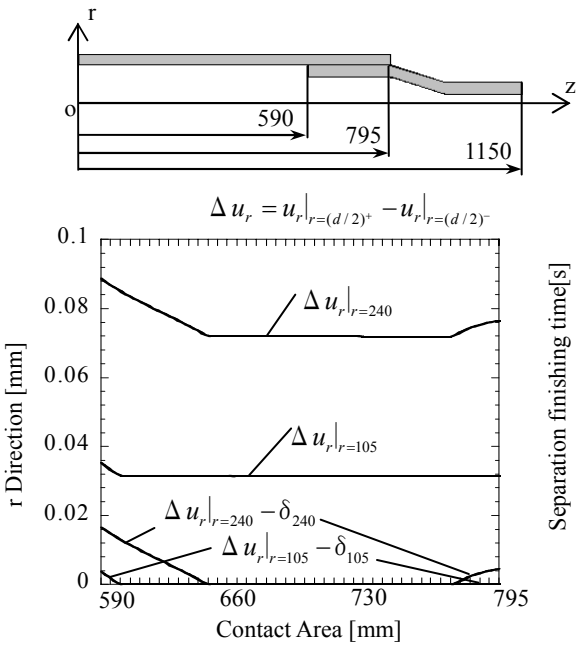

Fig.14 ΔU vs. Contact Area for D=270mm, 540mm (Time:1000 s, $\delta/d = 3.0\times10^{-4}$)

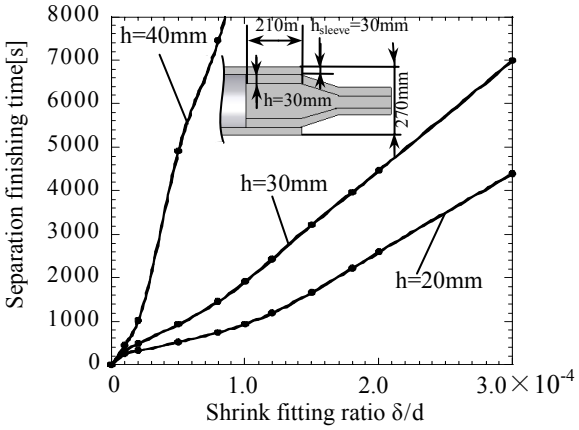

Fig.15 Time vs. δ/d for h=20mm,30mm,40mm

It is seen that when $\delta/d > 0.8\times10^{-4}$ for $h = 40mm$, the roller cannot be separated completely. In order to investigate the effect, the separation time becomes longer when the shaft thickness becomes larger similarly to the results for reducing the outside diameter D. Under the fixed sleeve thickness and diameter, larger shaft thickness h means smaller inner diameter of the shaft, which results in smaller water cooling effect. In this case, since the temperature difference between the sleeve and shaft becomes smaller, the separation becomes more difficult. Figure 16 shows the temperature differences $\Delta T = T_E - T_F$ when $\delta/d = 0.8\times10^{-4}$. Here, T_E is the temperature $T_E(z,r) = T_E(695,120)$, while T_F is $T_F(z,r) = T_F(695,90)$.It is seen that the temperature difference becomes smaller when the sleeve thickness is larger.

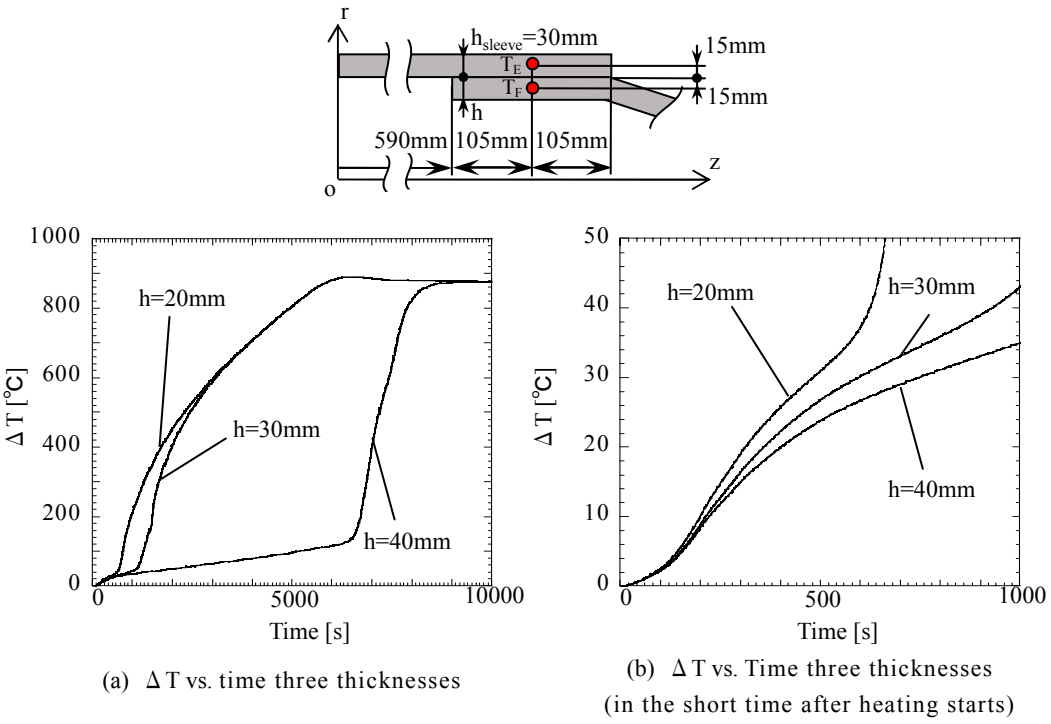

(a) ΔT vs. time three thicknesses

(b) ΔT vs. Time three thicknesses (in the short time after heating starts)

Fig.16 Temperature vs. Time for h=20mm, 30mm, 40mm($\delta/d=0.8\times10^{-4}$)

4.4 The Effect of Fitted Length L on Separation Time

Usually, the fitted length L in Fig.17 is designed to have a proportion to the inside diameter of the sleeve. If the fitted length is changed, the water cooing region is also changed. In this study, it is considered how the fitted length influences on separation time. Here, six fitted lengths are considered, $L = 100mm$, $L = 120mm$, $L = 140mm$, $L = 150mm$, $L = 180mm$ and the initial $L = 210mm$. In order to get the effect, the length of heated part is fixed as a constant value of 210mm, while water cooling part and air cooling part can be changed with fitted length.

Figure 17 shows the relationship between separation time and shrink fitting ratio for different fitted lengths. From Fig. 17, it is found that the separation time becomes smaller if L becomes shorter from $L = 210mm$. This is because short fitted length causes easy separation. However, Fig. 17 also indicates that if L becomes shorter than $L = 140mm$, the

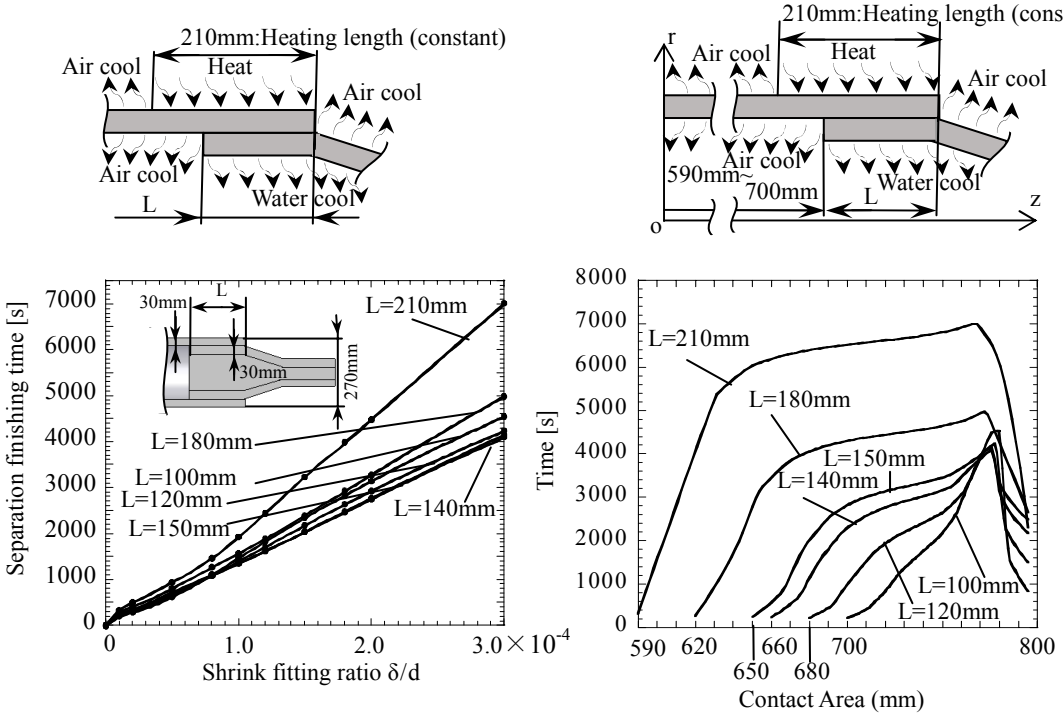

Fig.17 Time vs. δ/d for L=100mm,120mm,140mm,150mm,180 mm,210mm

Fig.18 Separation history of contact area for each L ($\delta/d=3.0\times10^{-4}$)

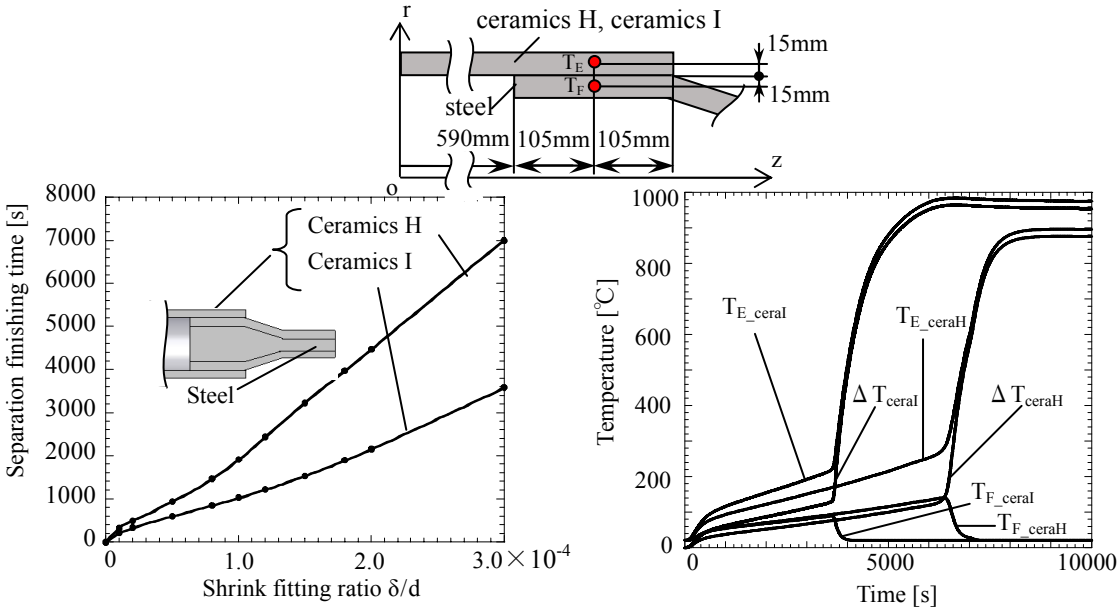

Fig.19 Time vs. δ/d when ceramics H sleeve, ceramics I sleeve

Fig.20 T_E, T_F and ΔT vs. Time for ceramics H sleeve, ceramics I sleeve

separation time becomes longer, which is because the effect of water cooling is also too small if L is too short.

Moreover, Fig. 18 shows the separation time along the contact region. From this figure, it is seen that separation starts from the shaft's end and next starts from the sleeve's end a bit later. The final separation point is on the inside of the contact region near the sleeve's end.

4.5 The Effect of the Thermal Conductivity of Sleeve on Separation Time

In this study, two kinds of ceramics in Table 2 are considered for the sleeve. Figure 19 shows separation time with varying the shrink fitting ratio. Obviously, separation time of ceramics H is longer than that of ceramics I. This is because the thermal conductivity of ceramics H is about 4 times larger than that of ceramics I. Figure 20 shows the temperature differences $\Delta T = T_E - T_F$ when $\delta/d = 0.3\times10^{-3}$. Here, T_E is the temperature $T_E(z,r) = T_E(695,120)$, while T_F is $T_F(z,r) = T_F(695,90)$. It is seen that the temperature difference becomes larger when thermal conductivity of sleeve becomes larger. The larger thermal conductivity causes larger temperature difference.

5. Conclusions

In this paper, for ceramics conveying rollers with ceramics sleeves and steel shafts of which inside is hollow, in order to exchange the shafts, the conditions to make them separate have been investigated. Different dimensions, shapes, materials and their effects on separation time have been discussed, which are shown in the following.

(1) Heating outside of the sleeve and cooling inside of the shaft by water are performed to make them separate. Separation of model A in Fig. 2 can not be realized, while it can be realized for model B with a thin shaft. Moreover, the separation time becomes shorter if the atmosphere temperature goes up more quickly or if the shrink fitting ratio becomes smaller (see Fig. 10, 11).

(2) The separation time becomes shorter if the outside diameter of the sleeve becomes larger (see Fig. 12).

(3) The separation time becomes shorter when the thickness of fitted part of the shaft becomes smaller (see Fig. 16), which is because the effect of water cooling becomes larger to make the temperature difference between shaft and sleeve rise difficultly.

(4) The separation times of different fitted lengths are investigated. It is found that the separation time becomes shorter if L becomes shorter from $L = 210mm$. However, when L becomes shorter than $L = 140mm$, the separation time becomes longer contrarily. In order to separate sleeve and shaft easily, $L = 140mm$ is the most suitable. In other words, the longest separation time appears for $L = 210mm$ and the shortest appears for $L = 140mm$.

(5) The separation time is short if the sleeve has a small value of heat conductivity, like ceramics I in this study (see Fig. 19, 20).

Reference

(1) Tsuyunaru, M., Noda, N-A., Hendra., and Takase, Y., “Maximum Stress for Shrink Fitting System Used for Ceramics Conveying Rollers”, *Transactions of the Japan Society of Mechanical Engineering*, Vol.74, No.743 (2008), pp.919-925; Noda, N-A., Hendra., Takase, Y., and Tsuyunaru, M., “Maximum Stress for Shrink Fitting System Used for Ceramics Conveying Rollers”, Journal of Solid Mechanics and Materials Engineering, Vol.2, No.11,2008.

(2) Iwata, T. and Mori, H., ”Material Choice for Hot Run Table Roller”, *Plant Engineer*, Vol.15, No.6 (1983), pp.55-59 (in Japanese) .

(3) Torii, K., “Heat Transfer Across the Solid Interface Governed by its Microscopic Surface-Structure –Interface between Macro-and Micro-Mechanics”, *The Japan Society of Mechanical Engineers*, Vol.96, No.892 (1993), pp.198-203 (in Japanese) .